

Electronic Supporting Information

Light-triggered NO release from a nanofibrous non-woven

Carmen Bohlender,^a Martin Wolfram,^a Helmar Goerls,^a Wolfgang Imhof,^e Roberto Menzel,^b Anja Baumgaertel,^{bc} Ulrich S. Schubert,^{bc} Ulrike Mueller,^d Martina Frigge,^d Matthias Schnabelrauch,^d Ralf Wyrwa,^d Alexander Schiller^{*ac}

^a Friedrich-Schiller-University Jena, Institute for Inorganic and Analytical Chemistry (IAAC), Humboldtstr. 8, 07743 Jena, Germany. Fax: +49 3641 948 102; Tel: +49 3641 948 113; E-mail: alexander.schiller@uni-jena.de

^b Friedrich-Schiller-University Jena, Laboratory for Organic and Macromolecular Chemistry (IOMC), Humboldtstr. 10, 07743 Jena, Germany

^c Friedrich-Schiller-University Jena, Jena Center for Soft Matter (JCSM), Humboldtstr. 10, 07743 Jena, Germany

^d INNOVENT e.V., Biomaterials Department, Pruessingstr. 27 B, 07745 Jena, Germany

^e University Koblenz-Landau, Institute for Integrated Natural Sciences, Universitätsstr. 1, 56070 Koblenz, Germany

Table of Contents

Materials, instruments and general procedures

Synthesis

X-Ray crystallography

Cyclovoltammetry

Mass spectrometry (MALDI-TOF MS)

Stability of Ru-NO complex **3 in hexafluoroisopropanol**

NO release studies

Photolysis Experiment

Ru-NO complex **3** in DMSO (Anslyn's fluorescent NO₅₅₀ probe)

Characterisation of non-wovens

MALDI-TOF MS

Energy dispersive X-ray spectrometry (EDX)

NMR

Leaching experiment

ICP-MS

Cytotoxicity

Photomicrographs of the non-woven **4b** with mouse fibroblasts 3T3

References

Materials, instruments and general procedures

Chemicals were obtained from Sigma Aldrich and VWR. Poly(L-lactide-co-D/L-lactide) 70/30 (PLA, Resomer LR 708, Boehringer Ingelheim, Germany) was used for electrospinning. A weight-average molar mass of $1.5 \times 10^6 \text{ g mol}^{-1}$ was determined for the polymer by size exclusion chromatography using CHCl_3 as solvent and polystyrene as external standard. Hexafluoroisopropanol (HFIP) was purchased from abcr (abcr GmbH & Co. KG, Karlsruhe, Germany) and used without further purification. Ethyl 1-methylimidazole-2-carboxylate was synthesized according to a literature procedure.¹ Synthesis of $\text{Ru}(\text{NO})\text{Cl}_3(\text{H}_2\text{O})_2$ was accomplished by an adapted mode of Fletcher *et al.*² $[(\text{bpb})\text{Ru}(\text{NO})(\text{Cl})]$ was synthesized following a modified protocol from Mascharak *et al.*³ The purity was checked via ^1H and ^{13}C NMR spectroscopy.

All solvents were purified and dried by a solvent purification system (Innovative Technology) prior to use. Standard Schlenk techniques (argon, nitrogen) were used during all syntheses to avoid exposure to dioxygen and moisture.

A microwave EM2 from LavisETHOS and standard reflux methods were used for the synthesis.

IR spectra were performed in a range of $400\text{--}4000 \text{ cm}^{-1}$ using KBr pellets using a Perkin Elmer System 2000 device and an IR-Affinity from Shimadzu.

Electrochemical measurements were performed on a Metrohm Autolab PGSTAT30 potentiostat with a standard three-electrode configuration using a graphite-disk working electrode, a platinum-rod auxiliary electrode, and an Ag/AgCl reference electrode. The experiments were carried out in degassed solvents containing $0.1 \text{ M Bu}_4\text{NPF}_6$ salt. At the end of the measurement, ferrocene was added as an internal standard.

UV-Vis spectra were recorded on an Analytik Jena Specord S 600 UV-Vis spectrometer.

Photocycles with UV-A excitation light were performed on a Cary 5000 UV-Vis/NIR spectrometer, equipped with a software controlled irradiation apparatus. The self made irradiation equipment consists of a 250 Watt maximum pressure mercury lamp in arrangement with a glass optic and a concave grid controlling the optical path of the emission wavelength. The excitation of the samples was performed at a 90° geometry related to the UV measure channel (distance of the grid to the cuvette chamber and the light source in each case 20 cm). The light intensity of the apparatus was determined using a $70 \mu\text{M}$ toluene solution of Aberchrome 540 as chemical actinometer, which was illuminated at $\lambda = 366 \text{ nm}$.⁴ UV/VIS spectra were taken after each 30 seconds of illumination calculating $I_0 = 3 \text{ mW/cm}^2$ by the method of Gade *et al.*⁵

LED excitation in a sealable illumination box was performed with a HD-LED module consisting of 5 vertically aligned LED lamps from INNOTAS Elektronik GmbH. The HD-LED module was placed in a fixed distance of 10 cm from a UV-Vis cuvette containing the determining complex together with an NO indicator in phosphate buffer (pH 7.4). To avoid external light interference, the illumination box was closed prior to every irradiation cycle. The intensity of the LED was calculated with the use of the Aberchrome 540 actinometer after photokinetic measurements as described above. ($I_0 = 2 \text{ mW/cm}^2$).

Fluorescence spectra were recorded on a Perkin Elmer LS50B luminescence spectrometer.

Mass spectra (EI, ESI) were obtained by the use of a Finnigan MAT SSQ 710 or MAZ95XL device. MALDI-TOF MS spectra were obtained using a Bruker Ultraflex III TOF/TOF instrument.

NMR spectra were recorded on a Bruker DRX 400 spectrometer (^1H : 400.13 MHz, ^{13}C : 100.62 MHz, solvent as internal standard).

Elemental analyses were performed utilising a CHNS-932 (LECO) at the Laboratory for Organic Chemistry and Macromolecular Chemistry, Friedrich-Schiller-University Jena.

Scanning electron microscopy (SEM) was performed with a field-emission scanning electron microscope Supra 55VP (Zeiss, Oberkochen, Germany). A Si wafer was used as substrate material for the fibres and Au was sputtered on the specimens to ensure a

sufficient electric conductivity for the analysis. The images were taken by the InLens-Detector using 5 keV excitation energy. The SEM is equipped with an energy dispersive X-ray spectroscopy (EDX) system Quantax with a Si(Li)-detector (Bruker, Berlin, Germany). The specimens were evaporated with Carbon. An excitation energy of 15 keV was used for the measurements. The spectra were taken from regions of the samples, where some fibres are crossed to have a larger excitation volume in the fibres for EDX.

ICP-MS measurements were performed on a XSeriesII from Thermo Fisher Scientific, Bremen.

The softwares Origin 8.5, MestReNova Lite, ChemDraw Ultra 12.0, Ortep3v2 and Mercury2.4 were used for visualisation of experimental data.

Synthesis

***N,N'*-(Ethane-1,2-diyl)bis(1-methyl-1*H*-imidazole-2-carboxamide) (1).** Ethyl 1-methylimidazole-2-carboxylate (1.0 g, 6.5 mmol) and 1,2-diaminoethane (220 μ L, 3.3 mmol) were dissolved in 1.0 mL (7.2 mmol) of triethylamine. The mixture was refluxed for 40 minutes with a microwave at 400 Watt under normal pressure. After evaporation of the solvent, a bright yellow oil was obtained. It was dissolved in 2 mL of a 1:1 mixture of ethyl acetate and diethyl ether and stored at -27 °C. The desired product precipitated as a white solid. It was filtered, washed with 10 mL of diethyl ether and dried in a vacuum (780 mg, yield: 87 %). ^1H NMR (CDCl_3 , 200 MHz): $\delta = 7.85$ (2H, s, NH), $\delta = 7.0$ (2H, d, $^3J = 1$ Hz, *H*-Im), $\delta = 6.94$ (2H, d, $^3J = 1$ Hz, *H*-Im), $\delta = 4.03$ (6H, s, CH_3), $\delta = 3.61$ (4H, t, $^2J = 2.7$ Hz, $^3J = 5.9$ Hz, CH_2). ^{13}C NMR (CDCl_3 , 200 MHz): $\delta = 159.6$ (2C, C=O), $\delta = 138.9$ (2C, $\text{C}_{q,2\text{Im}}$), $\delta = 127.6$ (2C, $\text{C}_{5\text{Im}}$), $\delta = 125.3$ (2C, $\text{C}_{4\text{Im}}$), $\delta = 38.9$ (2C, CH_2), $\delta = 35.5$ (2C, CH_3). FTIR (KBr disk, cm^{-1}): 3282 (NH-Amide, m), 3126 (C- H_{Im} , w), 2944 (C- H_{alkyl} , w), 1653 (Amide I, vs), 1558 (Amid II, vs), 1476, 1421 (C- H_{alkyl} , m), 1294, 1275 (γ_{alkyl} , s), 871 (C- H_{Im} , m). MS (DEI): m/z (%) = 277 (10) $[\text{M}+\text{H}]^+$, 151 (80) $[\text{M}-\text{C}_7\text{H}_7\text{N}_3\text{O}]^+$, 138 (92) $[\text{M}-\text{C}_6\text{H}_8\text{N}_3\text{O}]^+$, 109 (100) $[\text{M}-\text{C}_8\text{H}_{11}\text{N}_4\text{O}]^+$. EA for $\text{C}_{12}\text{H}_{16}\text{N}_6\text{O}_2$ calc.: C, 52.16; H, 5.84; N, 30.42 found: C, 52.16; H, 5.82; N, 30.36.

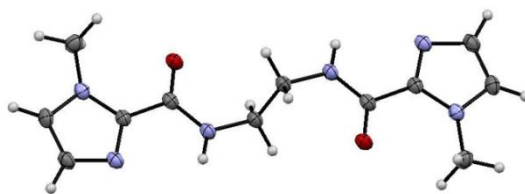


Fig. S1 Thermal ellipsoid plot (probability level 50%) of the molecular structure of *N,N'*-(ethane-1,2-diyl)bis(1-methyl-1*H*-imidazole-2-carboxamide) (1). Carbon is gray, oxygen red, nitrogen blue and hydrogen white.

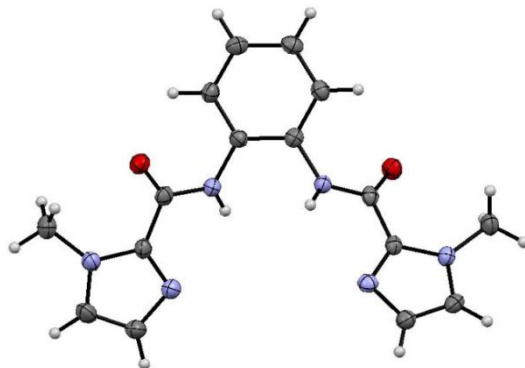


Fig. S2 Thermal ellipsoid plot (probability level 50%) of the molecular structure of *N,N'*-(1,2-phenylene)bis(1-methyl-1*H*-imidazole-2-carboxamide) (2). Carbon is gray, oxygen red, nitrogen blue and hydrogen white.

X-ray crystallography

Structure Determinations. The intensity data for the compounds were collected on a Nonius Kappa CCD diffractometer using graphite-monochromated Mo-K α radiation. Data were corrected for Lorentz and polarization effects but not for absorption effects.^{6,7} The structures were solved by direct methods (SHELXS⁸) and refined by full-matrix least squares techniques against Fo² (SHELXL-97⁸). All hydrogen atoms of **1** and for the amine groups of **2** was located by difference Fourier synthesis and refined isotropically. All other hydrogen atoms were included at calculated positions with fixed thermal parameters. All non-hydrogen atoms were refined anisotropically.⁸ Crystallographic data as well as structure solution and refinement details are summarized in Table S1. Ortep-3 for Windows (L. J. Farrugia) was used for structure representations.⁹

Crystallographic data (excluding structure factors) has been deposited with the Cambridge Crystallographic Data Centre as supplementary publication CCDC-818041 for **1**, CCDC-818042 for **2**, and CCDC-818043 for **3**. Copies of the data can be obtained free of charge on application to CCDC, 12 Union Road, Cambridge CB2 1EZ, UK [E- mail: deposit@ccdc.cam.ac.uk].

Table S1 Crystal data and refinement details for the X-ray crystal structure determinations.

Compound	1	2	3 ·C ₂ H ₃ N
formula	C ₁₂ H ₁₆ N ₆ O ₂	C ₁₆ H ₁₆ N ₆ O ₂	C ₁₆ H ₁₄ ClN ₇ O ₃ Ru·C ₂ H ₃ N
fw (g·mol ⁻¹)	276.31	324.35	529.92
T/°C	-140(2)	-140(2)	-140(2)
crystal system	monoclinic	triclinic	triclinic
Space group	P 21/c	P $\bar{1}$	P $\bar{1}$
a/ Å	10.3673(5)	11.4171(7)	8.0329(7)
b/ Å	14.6310(8)	11.8541(9)	10.7389(7)
c/ Å	9.1018(5)	12.1504(9)	12.3584(9)
α /°	90	81.797(4)	91.756(6)
β /°	105.698(3)	73.957(5)	97.964(4)
γ /°	90	75.363(5)	104.935(5)
V/Å ³	1329.10(12)	1524.40(19)	1017.69(13)
Z	4	4	2
ρ (g·cm ⁻³)	1.381	1.413	1.729
μ (mm ⁻¹)	0.99	0.99	9.41
measured data	8888	10391	7188
data with I > 2 σ (I)	2106	3950	3410
unique data (R _{int})	3032/0.0470	6870/0.0416	4605/0.0420
wR ₂ (all data, on F ²) ^{a)}	0.1098	0.1295	0.1104
R ₁ (I > 2 σ (I)) ^{a)}	0.0426	0.0538	0.0511
S ^{b)}	0.956	0.957	1.015
Res. dens./e·Å ⁻³	0.191/-0.307	0.246/-0.242	0.585/-0.934
absorpt method	NONE	NONE	NONE
CCDC No.	818041	818042	818043

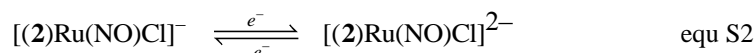
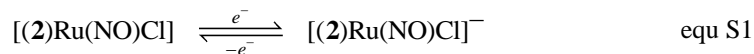
^{a)} Definition of the R indices: $R_1 = (\sum ||F_o| - |F_c||) / \sum |F_o|$;

$wR_2 = \{ \sum [w(F_o^2 - F_c^2)^2] / \sum [w(F_o^2)^2] \}^{1/2}$ with $w^{-1} = \sigma^2(F_o^2) + (aP)^2 + bP$; $P = [2F_c^2 + \text{Max}(F_o^2)]/3$;

^{b)} $S = \{ \sum [w(F_o^2 - F_c^2)^2] / (N_o - N_p) \}^{1/2}$.

Cyclic voltammetry

The cyclic voltammetric scans of complex **3** are shown in Figure S3. Due to the extreme low solubility the experiment had to be carried out in DMSO or DMF which exhibit only a small electrochemical window especially for the oxidation side. The cyclic voltammogram, measured against the internal standard ferrocene/ferrocenium (Fc/Fc⁺), revealed two electrochemical processes. In DMSO, the first reduction (A) is reversible (see inset Figure S3 left) with a half-wave potential of $E_{1/2} = -0.91$ V ($\Delta E = E_{pa} - E_{pc} = 192$ mV). In DMF, the first reduction wave (A) is also reversible (see inset Figure S3 right) with a half-wave potential of $E_{1/2} = -1.04$ V ($\Delta E = 91$ mV). This processes can be assigned to the reduction of the nitrosyl cation leading to the formation of a negatively charged complex (equ S1).¹⁰ The measured potential is consistent compared to similar example complexes from literature.^{3,11,12}



In DMSO, the second reduction at $E \approx -1.60$ V (B) is irreversible and could lead to a negatively charged complex (equ S2).¹³

In contrast, the second reduction (B) in DMF is reversible with a half-wave potential of $E_{1/2} = -1.54$ V ($\Delta E = 92$ mV).¹³ The two measured potentials of the reduction in DMSO and DMF (A and B) are more negative compared to the reference complex [(bpb)Ru(NO)(Cl)] ($\text{H}_2\text{bpb} = 1,2\text{-bis(pyridine-2-carboxamido)benzene}$)³ with $E_1 = -0.17$ V and $E_2 = -0.64$ V vs SCE¹¹ or to the complex [(Me₂bpb)Ru(NO)(Cl)] ($\text{H}_2\text{Me}_2\text{bpb} = 1,2\text{-bis(quinaldine-2-carboxamido)-4,5-dimethylbenzene}$) with $E_1 = -0.46$ V vs SCE (Fc/Fc⁺ vs SCE ≈ 0.49 V).^{3,12,14}

An irreversible weak oxidation wave (C) located at $E = 0.66$ V as estimated from DPP measurements can be observed in DMSO. This could be assigned to the oxidation of the Ru(II) center to Ru(III) to form complex [(2)Ru(NO)(Cl)]⁺. Finally, also no clear oxidation behavior of **3** was apparent in DMF (a small shoulder is present at 0.58 V but the assignment from DPP measurements was tentative, Fig. S3 right).

It is noteworthy that the presented potentials cannot be compared directly because of the use of different reference systems and measurement conditions but they clearly show the similarity (e.g. two distinct reduction peaks) between complex **3** and [(bpb)Ru(NO)(Cl)].

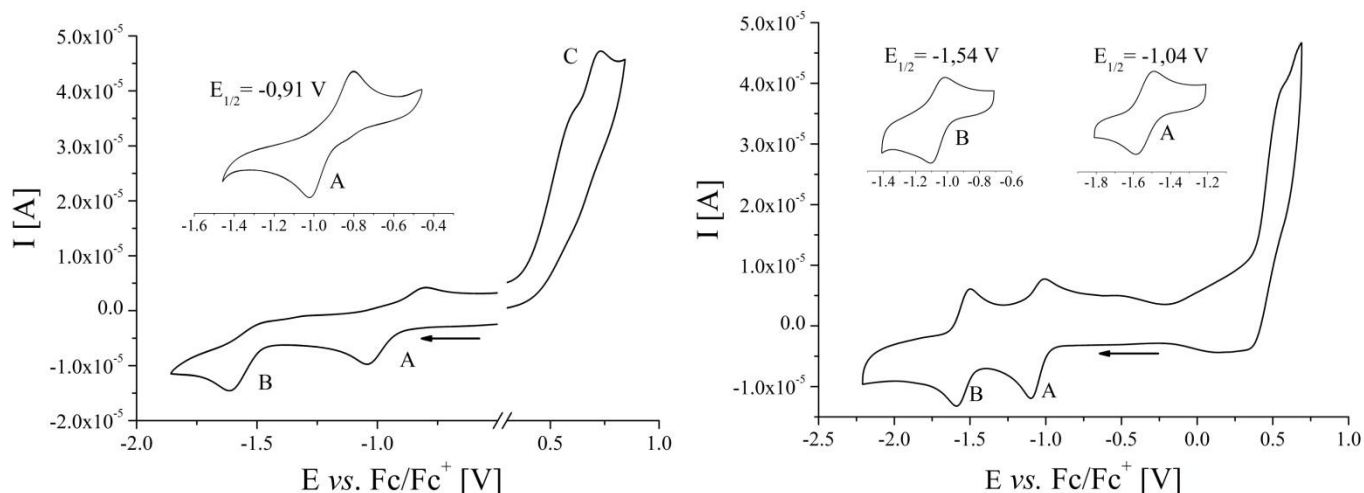


Fig. S3 Cyclic voltammetry of **3** in DMSO (left) and DMF (right). Experimental conditions: 0.1 M TBAPF₆, [Ru] 4×10^{-4} M (left), [Ru] 1.5×10^{-3} M (right), 25°C, 200 mV/s⁻¹, RE: Ag/AgCl, WE: carbon, AE: platinum.

Mass spectrometry

All MALDI-TOF MS spectra were measured in the positive reflector mode. The instrument was calibrated prior to every measurement with an external standard in the required m/z region. As preparation techniques, the dried-droplet method was chosen.¹⁵ Therefore, a certain amount of the sample solution as well as the matrix solution was mixed together and 1 μL of the gained mixture was deposited on the MALDI target.

The obtained MALDI-TOF MS spectrum revealed several signals without the chloride ion containing the desired Ru-NO complex structure at m/z 454 as well as the fragmented Ru complex without the labile NO group at m/z 424. In addition, bis-complexes consisting of the fragmented Ru complex with or without the counter ion are visible at m/z 848 and 882, respectively.

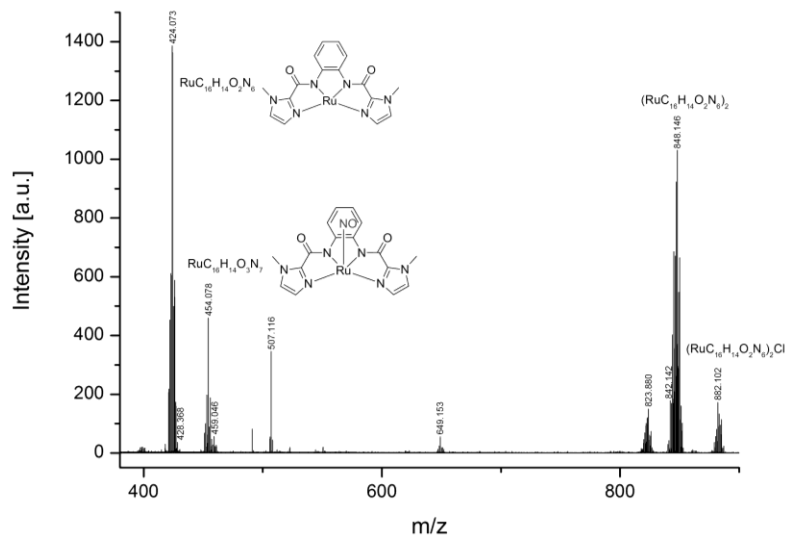


Fig. S4 MALDI-TOF MS spectrum of **3** (matrix: dithranol in chloroform; spotting technique: dried-droplet method).

Stability of **3** in hexafluoroisopropanol (solvent for electrospinning)

Complex **3** was dissolved in hexafluoroisopropanol at room temperature. After 2 hours, the solvent was evaporated. The residue was checked by ^1H NMR in DMSO-d_6 and showed identical signals as untreated **3**.

NO release

Photolysis Experiment

Photocycles with UV-A excitation light ($\lambda = 366$ nm) were performed on a Cary 5000 UV-Vis/NIR spectrometer, equipped with a 250 W mercury lamp (3 mW/cm²). The cuvette was held at a fixed distance of 20 cm from the grid in the illumination apparatus. Absorption spectra were taken after each irradiation for a certain period of time. Absorbance values at a specific wavelength (432 nm for **3**) were obtained from the respective spectra, and observed rate constant values (k_{NO}) were obtained by fitting the absorbance values to the equation $A(t) = A_{\infty} + (A_0 - A_{\infty})e^{-k_{\text{NO}} \cdot t}$, where A_0 and A_{∞} are respectively the initial and final absorbance values at the fixed wavelength. The rate constant is the mean value of three independent measurements. The errors are within a 10% range.

Ru-NO complex **3** in DMSO with Anslyn's NO₅₅₀ probe¹⁶

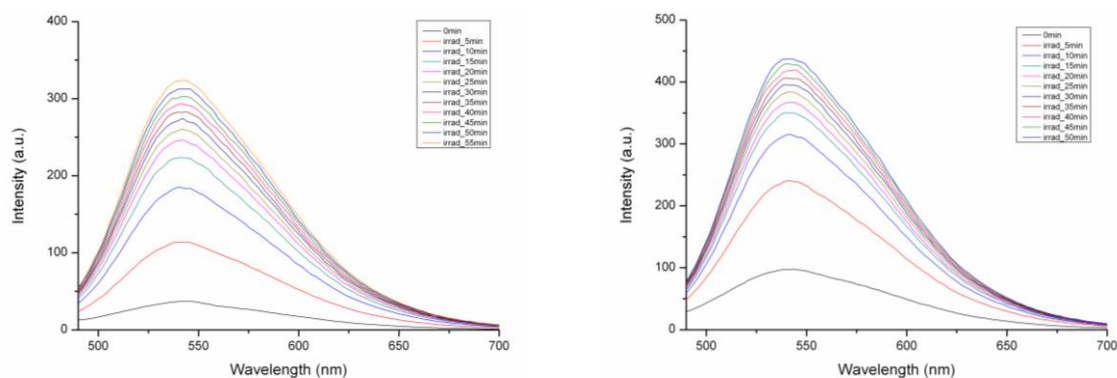


Fig. S5. Emission spectra ($\lambda_{\text{ex}} = 470$ nm) of 9-(dimethylamino)dibenzo [c,h]cinnoline-1-carbonitrile (reaction product of 5-amino-6-(3-(dimethylamino)phenyl)-1-naphthonitrile with NO, 10 μM left, 30 μM right) obtained every 5 min when **3** (10 μM left and 30 μM right) was irradiated with UV-A light ($\lambda_{\text{exc}} = 366$ nm) in aerobic DMSO. Overall reaction time was 55 min.

Characterization of the non-wovens **4a** and **4b**

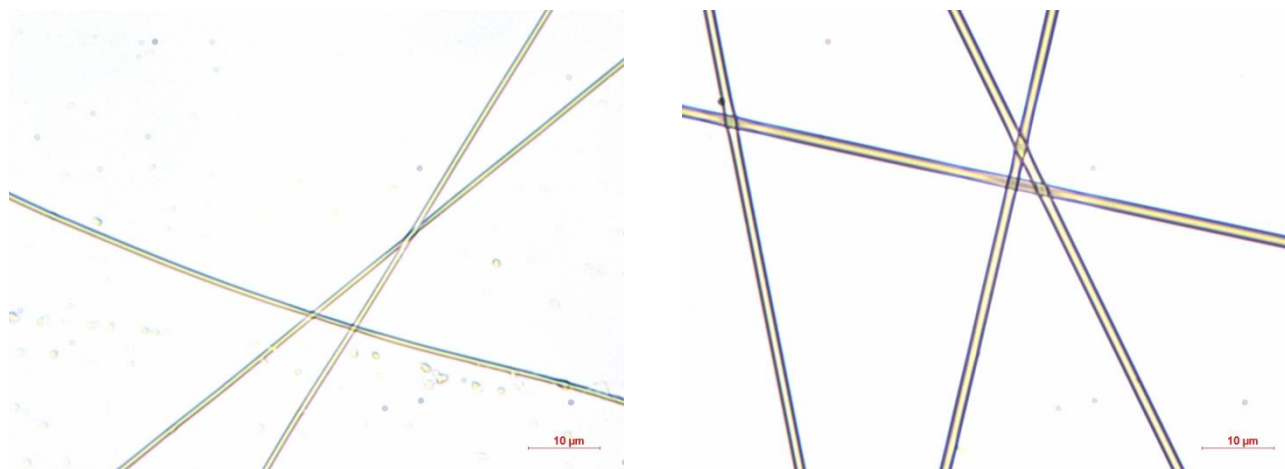


Fig. S6. Lightmicroscopy pictures of single nanofibres of **4a** (left) and **4b** (right).

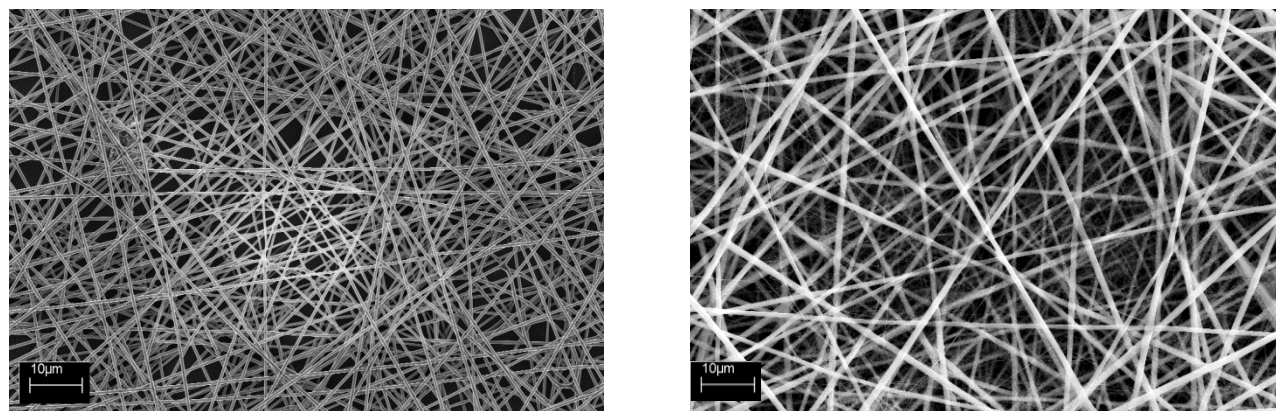


Fig. S7. SEM images of electrospun PLA nanofibrous non-wovens **4a** (left) and **4b** (right). White bar represents 10 μm .

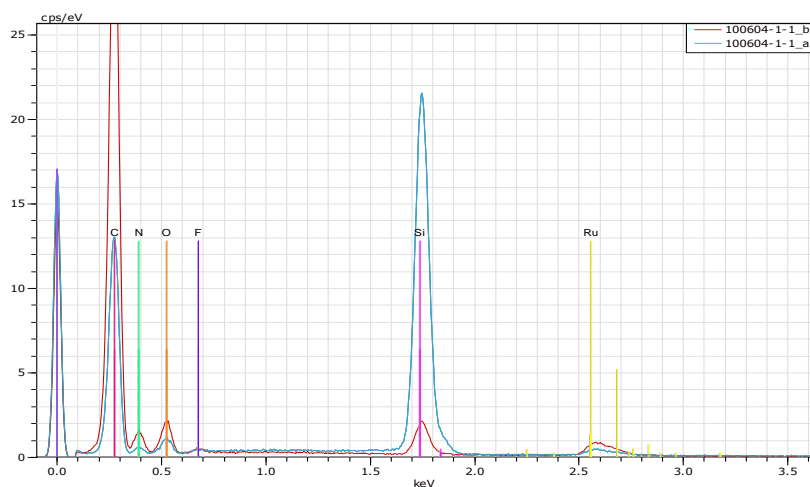


Fig. S8. EDX spectra of **4a** (blue line) and **4b** (red line).

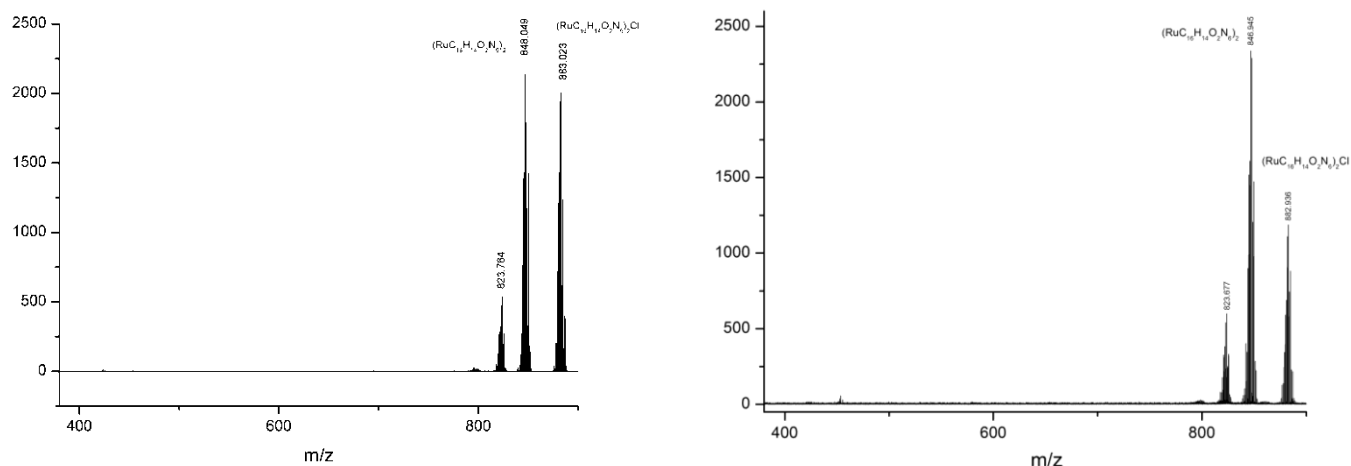


Fig. S9. MALDI-TOF MS spectra of **4a** (left) and **4b** (right) (matrix: 2,5-dihydroxybenzoic acid; spotting technique: multiple-layer spotting method).

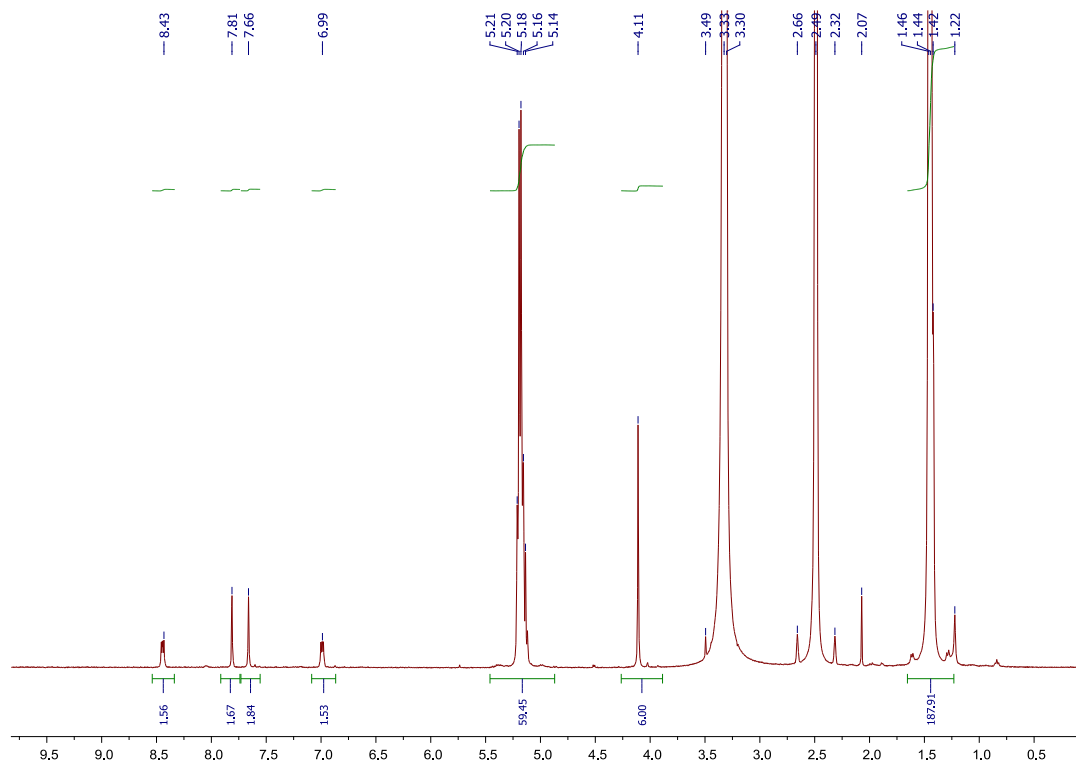


Fig. S10. ^1H NMR (400 MHz) of **4a** dissolved in DMSO-d_6

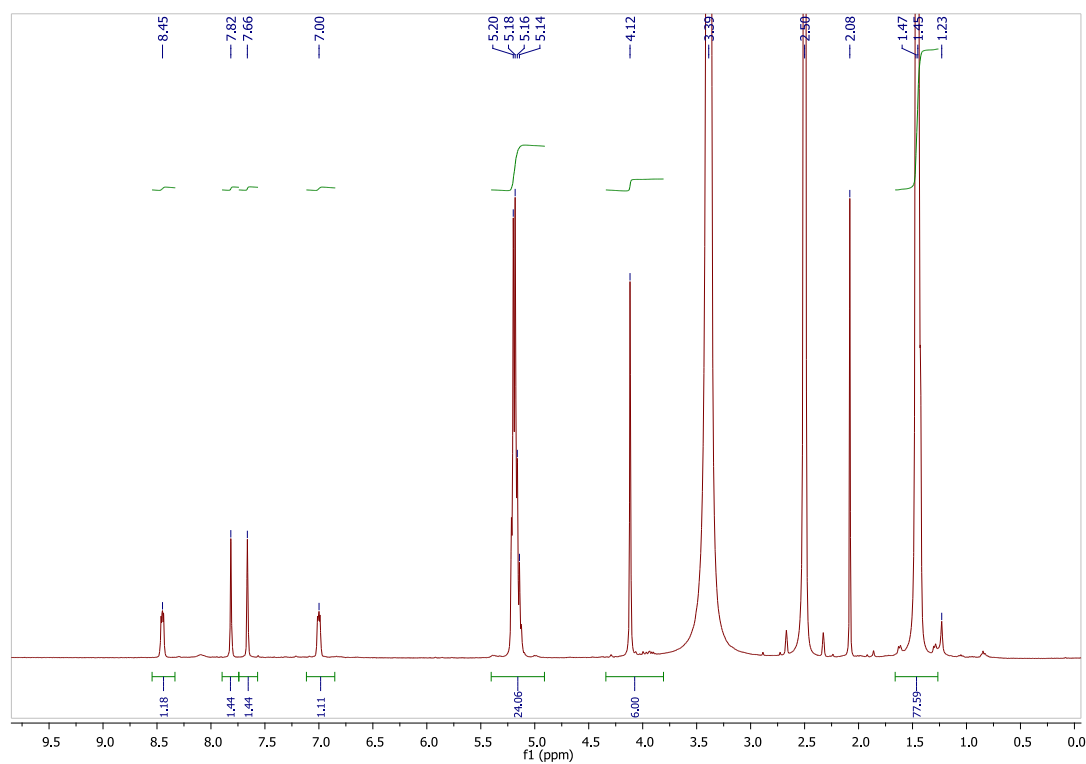


Fig. S11. ^1H NMR (400 MHz) of **4b** dissolved in DMSO-d_6

Table S2. Calculation of the content of **3** in PLA nanofibres **4a** and **4b** by ^1H NMR (see Fig. S10 and S11).

	Non-woven 4a (10 wt% of 3 in PLA)	Non-woven 4b (25 wt% of 3 in PLA)
^1H NMR integral values from the methyl group of 3	6.00	6.00
^1H NMR integral values from the methyl group of PLA	187.91	77.59
Calculated content Complex 3 : M 488.85 g/mol PLA: M 72.06 g/mol	11 wt%	26 wt%

Leaching experiment

A sample of **4b** ($m = 0.7$ mg of **4b**, 25 wt% of **3** ($M = 488.85$ g mol $^{-1}$) $\rightarrow m(\mathbf{3}) = 0.18$ mg, $n(\mathbf{3}) = 0.36$ μmol) was fixed on a paper clip. The clip was immersed in pure water ($V = 2.5$ mL) at room temperature. The resulting concentration of **3** was 0.14 mM if it were soluble. Absorbance spectra of the supernatant were recorded from 3 h to 8 days (Fig. S12). Only a very small amount of **3** (1.4 % from **4b**, 0.2 % after 3 h!) was identified in the aqueous phase after 8 days due to the very low solubility of **3**. Here, an approximated extinction coefficient $\varepsilon_{345} = 14,100$ M $^{-1}\text{cm}^{-1}$ (usually measured in DMF, see Fig. 2) was used to calculate the concentration of **3** from the absorbance.

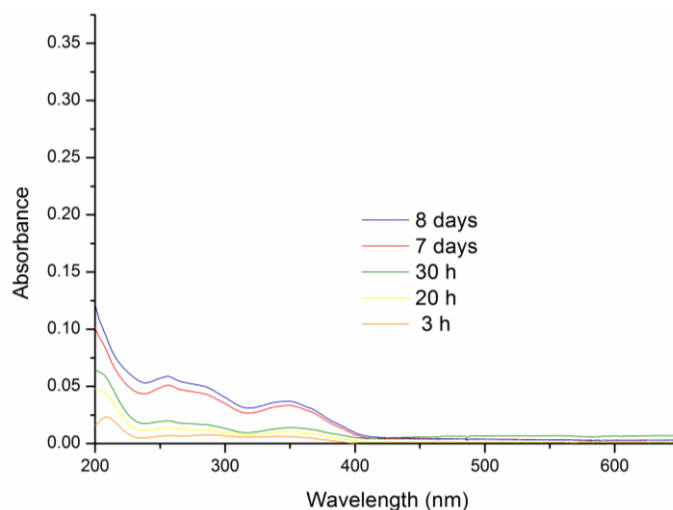


Fig. S12. Absorbance spectra of the supernatant of the 25 wt% non-woven **4b** in pure water in a “leaching experiment”. **4b** on a paper clip was immersed at room temperature. Absorbance spectra of the supernatant were recorded from 3 h to 8 days. Only a very small amount of **3** can be identified in the aqueous phase after 8 days due to the very low solubility of **3** in water.

Leaching verified by ICP-MS measurements

To determine the rate of leaching of the complex from the non-woven **4b** (25 wt% of Ru complex **3**) in given time intervals, samples of the non-woven were accurately weighed and kept in MilliQ water (2.5 or 10 mL) for three hours, one day and five days.

Another set of samples was irradiated at 366 nm for three hours (in a volume of 2.5 mL) before storing the samples in 2.5 mL MilliQ water for three hours, one day and five days. After removing the non-wovens from the aqueous solutions, concentrated nitric acid was added and filled up with MilliQ water to reach a final nitric acid concentration of 4%. To quantify the ruthenium content within the leaching solutions, ICP-MS measurements were performed on a XSeriesII from Thermo Fisher Scientific, Bremen (Isotop 101 Ru). For calibration and measurement 10 mg/L of Re was used for drift correction.

Table S3. ICP-MS analysis of the leaching experiment of **4b**.

Exp.	Weight of 4b (mg)	Weight of Ru (µg)	Estimated leaching rate (%)	Estimat. conc. (µg/l)	Meas. conc. (µg/l)	Stand. dev. (µg/l)	Calculated leaching rate (%)	Calculated leaching rate irradiation (%)	Leaching volume	Leaching time	Comment
1A	0,98	50,65	0,10	9,80	19,64	0,04	0,20		2,5 mL	3h	weight ratio ~2500
1B	0,79	40,83	0,10	7,90	23,40	0,40	0,30	3h			
2A	0,90	46,52	0,40	36,01	9,78	0,07	0,11	1d			
2B	1,12	57,89	0,40	44,82	8,80	0,20	0,08	1d			
3A	0,95	49,10	2,00	190,06	12,00	0,00	0,13	5d			
3B	1,10	56,86	2,00	220,08	8,00	0,30	0,07	5d			
4A	1,21	62,54	0,10	5,14	35,93	0,02	0,70	10 mL	3h	weight ratio ~10000	
4B	1,03	53,24	0,10	4,38	41,90	0,60	0,96		3h		
5A	1,01	52,20	0,40	17,16	25,30	0,20	0,59		1d		
5B	1,14	58,92	0,40	19,37	6,60	0,07	0,14		1d		
6A	0,99	51,17	2,00	84,11	3,08	0,01	0,07		5d		
6B	0,89	46,00	2,00	75,61	20,60	0,10	0,54		5d		
7A	0,84	43,42		8,40	4,50	0,10		0,05	2,5 mL		180 min irradi.
7B	0,84	43,42		8,39	15,30	0,30	0,18			3h	180 min irradi.
8A	0,96	49,62		10,26	5,72	0,08		0,06			180 min irradi.
8B	0,96	49,62		9,59	11,90	0,00	0,12			3h	180 min irradi.
9A	1,14	58,92		11,40	16,30	0,20		0,14			180 min irradi.
9B	1,14	58,92		45,57	30,10	0,50	0,26			1d	180 min irradi.
10A	0,95	49,10		9,50	2,10	0,10		0,02			180 min irradi.
10B	0,95	49,10		37,97	9,90	0,20	0,10			1d	180 min irradi.
11A	1,00	51,69		10,00	12,60	0,10		0,13			180 min irradi.
11B	1,00	51,69		199,87	34,70	0,20	0,35			5d	180 min irradi.
12A	1,08	55,82		10,80	3,80	0,10		0,04			180 min irradi.
12B	1,08	55,82		215,86	17,09	0,00	0,16			5d	180 min irradi.
13	0,62	0,00		0,00	0,01	0,00					Non-woven blank

Cytotoxicity

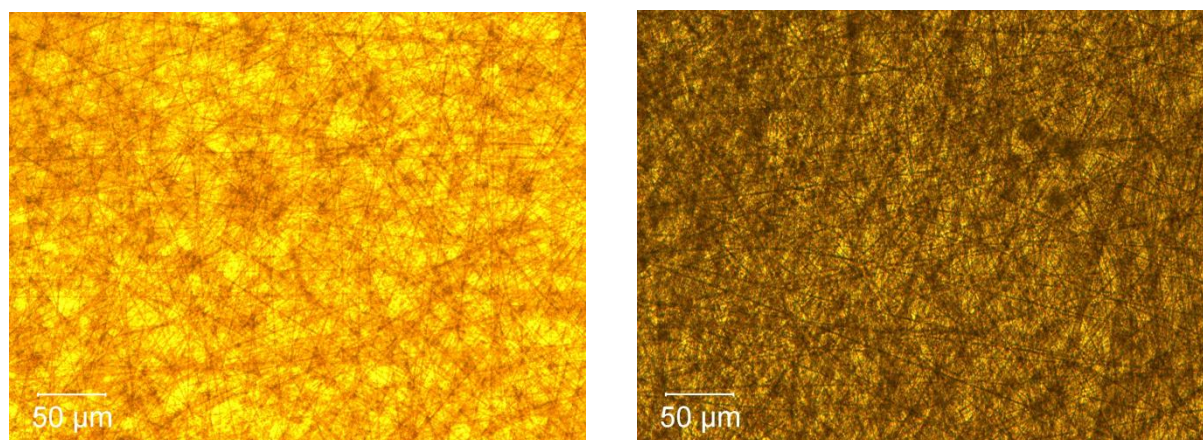


Fig. S13. Photomicrographs of the non-woven **4b** with mouse fibroblasts 3T3 after 1 day (left) and 4 days (right).

References

1. E. E. Baird and P. B. Dervan, *J. Am. Chem. Soc.*, 1996, **118**, 6141-6146.
2. J. M. Fletcher, I. L. Jenkins, F. M. Lever, F. S. Martin, A. R. Powell and R. Todd, *J. Inorg. Nucl. Chem.*, 1955, **1**, 378-401.
3. A. K. Patra, M. J. Rose, K. A. Murphy, M. M. Olmstead and P. K. Mascharak, *Inorg. Chem.*, 2004, **43**, 4487-4495.
4. H. G. Heller and J. R. Langan, *J. Chem. Soc., Perkin Trans. 2*, 1981, 341-343.
5. R. Gade and T. Porada, *J. Photochem. Photobiol., A*, 1997, **107**, 27-34.
6. B. V. Nonius, *COLLECT, Data Collection Software*, Netherlands, 1998.
7. Z. Otwinowski and W. Minor, in *Methods in Enzymology, Macromolecular Crystallography, Part A*, eds. C. W. Carter and R. M. Sweet, Academic Press, 1997, vol. 276, pp. 307-326.
8. G. M. Sheldrick, *Acta Cryst.*, 2008, **A64**, 112-122.
9. L. J. Farrugia, *J. Appl. Cryst.*, 1997, **30**, 565.
10. R. W. Callahan and T. J. Meyer, *Inorg. Chem.*, 1977, **16**, 574-581.
11. Z. N. Zahran, D. R. Powell and G. B. Richter-Addo, *Inorg. Chim. Acta*, 2006, **359**, 3084-3088.
12. D. R. Lang, J. A. Davis, L. G. F. Lopes, A. A. Ferro, L. C. G. Vasconcellos, D. W. Franco, E. Tfouni, A. Wieraszko and M. J. Clarke, *Inorg. Chem.*, 2000, **39**, 2294-2300.
13. M. G. Sauaia and R. S. da Silva, *Transition Met. Chem.*, 2003, **28**, 254-259.
14. P. Zanello, *Inorganic Electrochemistry: Theory, Practice, and Application*, The Royal Society of Chemistry, Cambridge, 2003.
15. H. Räder and W. Schrepp, *Acta Polym.*, 1998, **49**, 272-293.
16. Y. Yang, S. K. Seidlits, M. M. Adams, V. M. Lynch, C. E. Schmidt, E. V. Anslyn and J. B. Shear, *J. Am. Chem. Soc.*, 2010, **132**, 13114-13116.